

In-situ calibration and linearity with  $Z \rightarrow ee$   
&  
Double Higgs production in  $b\bar{b} \gamma\gamma$  final state  
in ATLAS

Linghua Guo

IJCLab  
17/05/2021

# Introduction

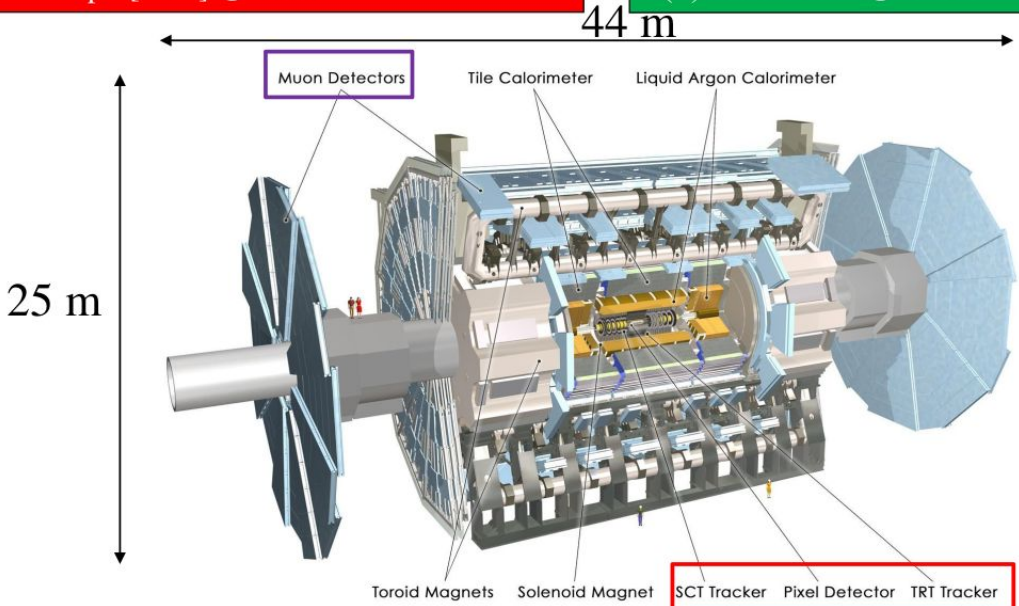
Thesis work mainly about two parts:

- **ATLAS electromagnetic calorimeter calibration and non-linearity**
  - In-situ calibration of calorimeter using  $Z \rightarrow ee$  events
  - Reduce non-linearity systematic uncertainty, crucial for  $H \rightarrow$  diphoton mass measurement
- **Double Higgs production in two b-jets and two photons final state**
  - SM Higgs self-coupling
  - BSM: exotic self-coupling, new resonant particle

# ATLAS experiment

**1**  
Inner Detector ( $|\eta| < 2.5$ ,  $B=2$  T)  
 Si pixels, strips, Transition Radiation Tracker  
 Tracking, vertexing,  $e/\pi$  separation  
 $\sigma(p_T)/p_T < 3.8 \cdot 10^{-4}$  pT [GeV]  $\oplus$  0.015

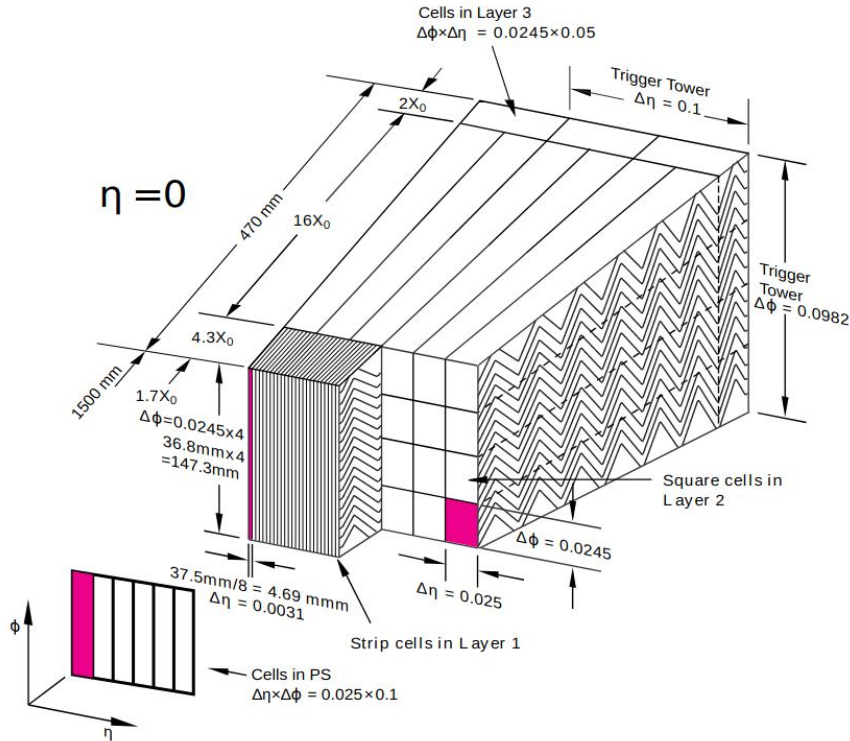
**2**  
EM Calorimeter ( $|\eta| < 3.2$ )  
 Pb-LAr accordion, longitudinal segmentation  
 $e/\gamma$  separation  
 $\sigma(E)/E \approx 10\%/\sqrt{E} \oplus 0.7\%$



**3**  
Hadronic Calorimeter  
 Fe-scint. ( $|\eta| < 1.7$ ) ; Cu-LAr  $1.5 < |\eta| < 3.2$   
 Cu/W -LAr (fwd) :  $3.1 < |\eta| < 4.9$   
 Trigger, jet, MET ;  $\sigma(E)/E \approx 50\%/\sqrt{E} \oplus 3\%$

**4**  
Muon Spectrometer ( $|\eta| < 2.7$ )  
 Air core toroid magnets (0.5-1 T), gas chambers  
 $\mu$  trigger and momentum measurement  
 $\sigma(p_T)/p_T = 2\%$  at 50 GeV ;  $10\%$  at 1 TeV

# ATLAS EM calorimeter (ECAL)



Sampling calorimeter:

**Lead** as absorber, **liquid Argon** as active material

**4 layer structure (sampling):**

**Presampler:**

estimate energy loss before “accordion”

**Strip:**

high granularity strip separates neutral pion and converted photons

**Middle:**

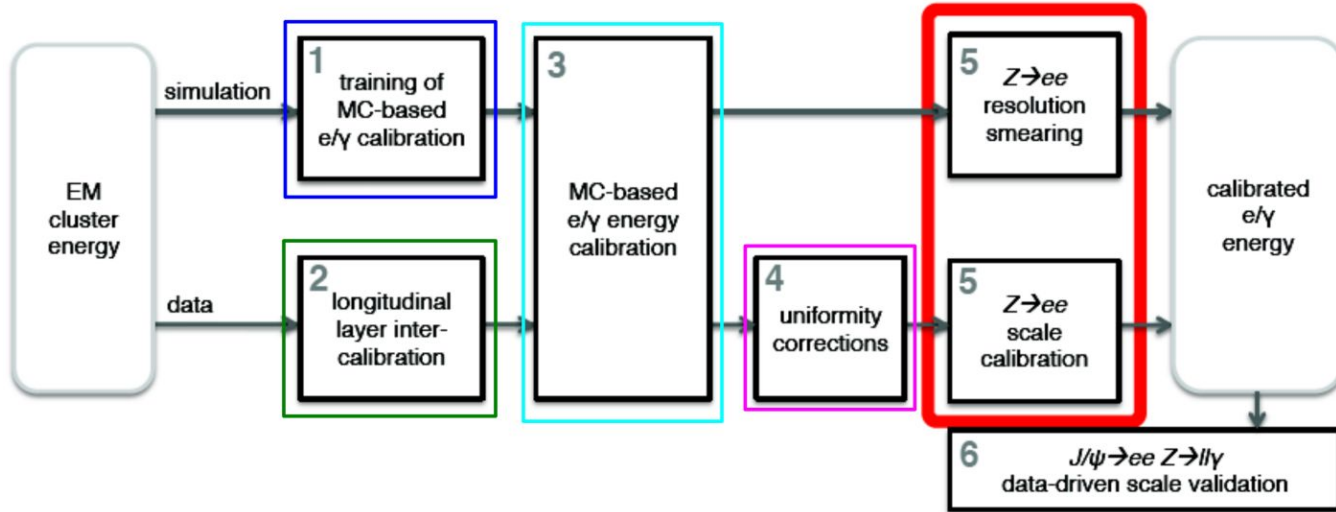
contains most of the shower

**Back:**

longitudinal leakage

Accurate **calibration** required for this complex detector.

# ECAL calibration



- **MVA calibration:**  
regression, reconstructed energy to truth energy in MC, applied on both data and MC
- **Layer intercalibration:**  
rebalance relative energy response **Strip/Middle** between data and MC
- **Zee in-situ calibration:**  
calibrate residual data-MC difference with **Z mass peak** (well known process with resonant mass around 91 GeV)  
diff. arise from electronic mis-calibration, mis-modeling of detector geometry, LAr temperature, etc...

# Zee calibration and linearity measurement

After step 4, remaining difference Data vs MC:  
**1% difference of scale, 0.5% difference on resolution.**

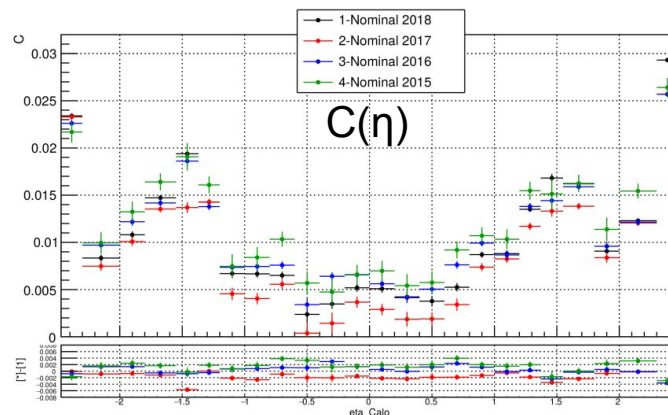
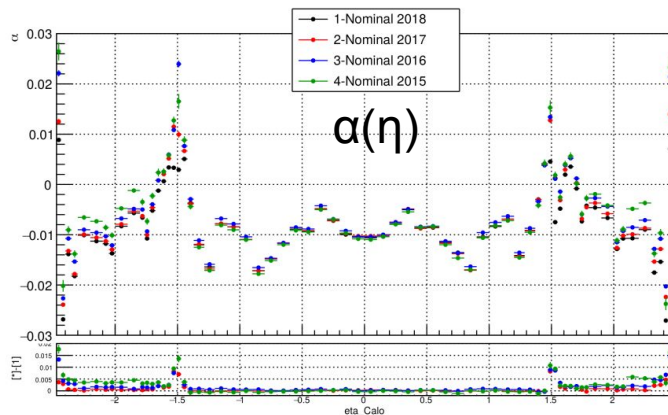
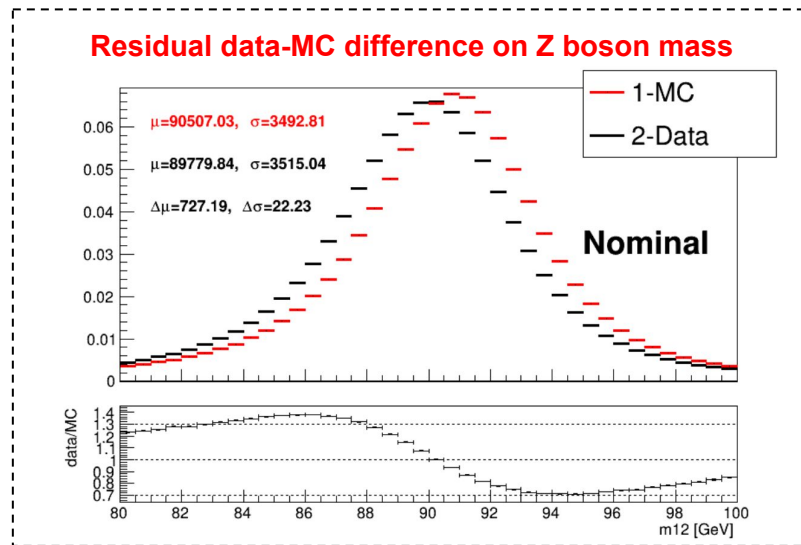
Parameterize data-MC difference in function of pseudorapidity ( $\eta$ ):

- $\alpha(\eta)$ : scale correction

$$E^{data} = E^{MC} (1 + \alpha(\eta^{calo}))$$

- $C(\eta)$ : resolution correction, Gaussian smearing

$$\left(\frac{\sigma(E)}{E}\right)^{data} = \left(\frac{\sigma(E)}{E}\right)^{MC} \oplus C(\eta^{calo})$$



# Higgs mass precision measurement

## H→diphoton analysis

### Breakdown of Higgs mass systematic uncertainties

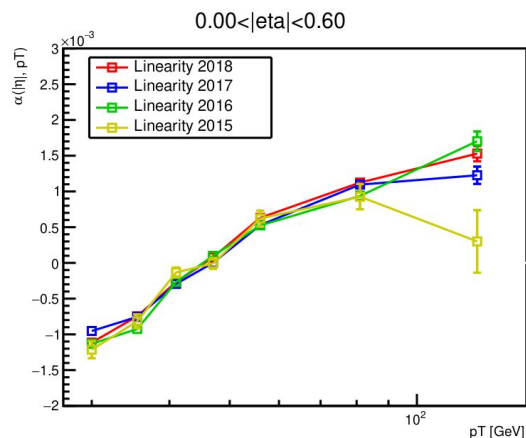
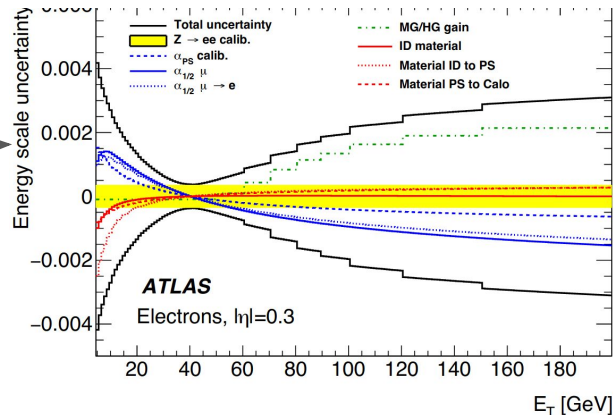
Source	Systematic uncertainty on $m_H^{\gamma\gamma}$ [MeV]
EM calorimeter cell non-linearity	$\pm 180$
EM calorimeter layer calibration	$\pm 170$
Non-ID material	$\pm 120$
ID material	$\pm 110$
Lateral shower shape	$\pm 110$
Z → ee calibration	$\pm 80$
Conversion reconstruction	$\pm 50$
Background model	$\pm 50$
Selection of the diphoton production vertex	$\pm 40$
Resolution	$\pm 20$
Signal model	$\pm 20$

### Exploit energy-dependent scale correction with Zee:

$$E^{data} = E^{MC}(1 + \alpha(\eta^{calo}))(1 + \alpha'(|\eta^{calo}|, p^T))$$

Consider it as measurements of all non-linearity systematic effect

ECAL non-linearity: dominant systematic uncertainty of Higgs mass with two photon



Preliminary results: factor ~ 2 reduction of uncertainty thanks to constrain and correlation

# ATLAS Run2 Higgs pair production in $b\bar{b}\gamma\gamma$ final state



Run: 329964  
Event: 796155578  
2017-07-17 23:58:15 CEST



# Physics motivation

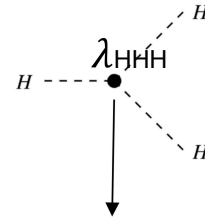
$$\mathcal{L}_{\text{Higgs}} = (D_\mu \Phi)^\dagger (D_\mu \Phi) - \left( \mu^2 \Phi^\dagger \Phi + \lambda (\Phi^\dagger \Phi)^2 \right)$$

after spontaneous symmetry breaking

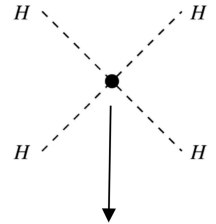
$$\supset \delta V m_V^2 V_\mu V^\mu \left( 1 + \frac{H}{v} \right)^2 - \lambda v^2 H^2 \left( 1 + \frac{H}{2v} \right)^2$$

$$m_H = \sqrt{2\lambda v^2}, \lambda_{\text{HHH}} = 6\lambda v, \lambda_{\text{HHHH}} = 6\lambda$$

$$\lambda \approx 0.13 \text{ with } v \approx 246 \text{ GeV}, m_H \approx 125 \text{ GeV}$$

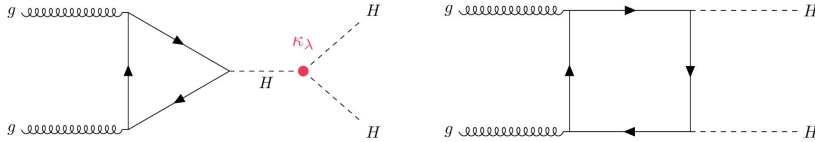


Direct access in  
HH pairs



Out of reach  
even for HL-LHC

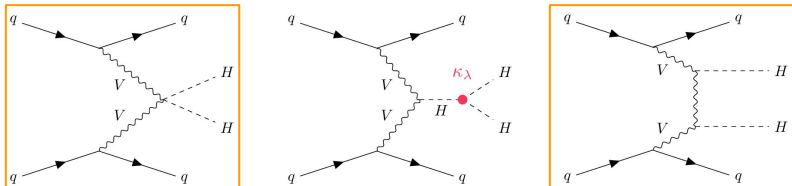
Non resonant ggF:  $\sigma_{\text{SM}} = 31.02 \text{ fb}$  at 13 TeV for  $m_H = 125.09 \text{ GeV}$



Self-coupling modifier  $\kappa_\lambda = \lambda_{\text{HHH}} / \lambda_{\text{HHH}}^{\text{SM}}$

Tiny cross section ( $\sim \sigma_H / 1000$ )

Non resonant VBF:  $\sigma_{\text{SM}} = 1.72 \text{ fb}$  at 13 TeV for  $m_H = 125.09 \text{ GeV}$



ggF production:

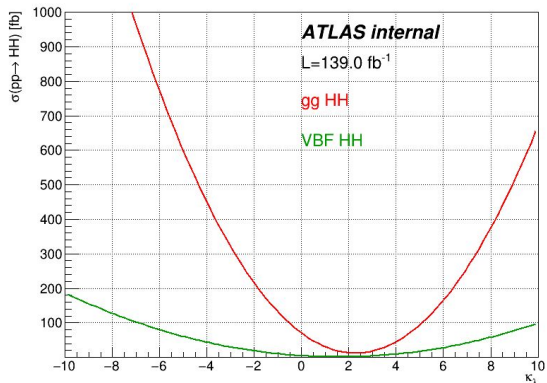
negative interference between triangle and box

VBF production:

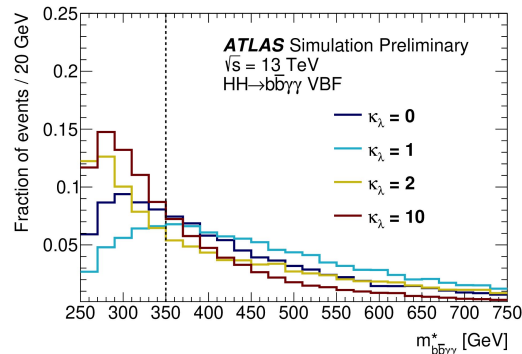
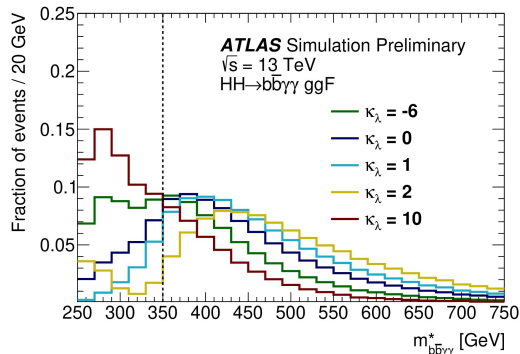
large **suppression** between VVHH and VVH

# Motivation to new physics

**Anomalous self-coupling:**  $\sigma$  increases with  $|\kappa_\lambda|$   
 → possible sensitivity with Run 2 data

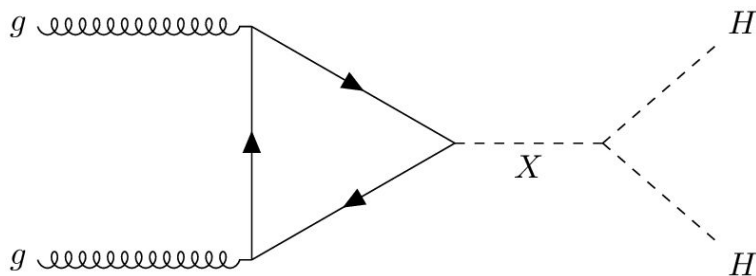


$\kappa_\lambda - m_{HH}$  correlation: Inspiration for categorization



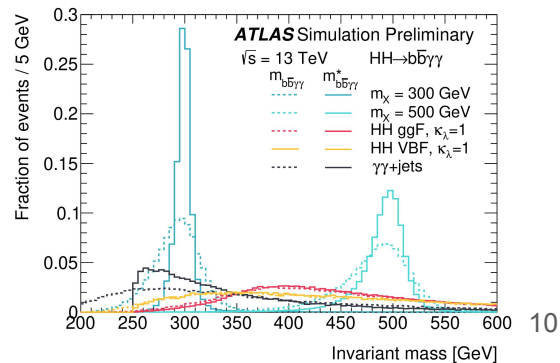
$$m_{bb\gamma\gamma}^* = m_{bb\gamma\gamma} - m_{b\bar{b}} - m_{\gamma\gamma} + 250 \text{ GeV}$$

**Search of resonant scalar:**




**Scalar:**

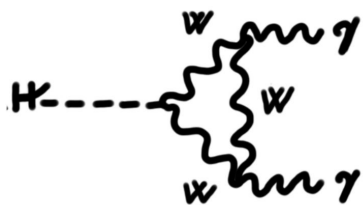
- $m_X$  in [251, 1k] GeV
- Narrow width approximation



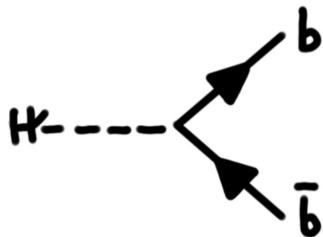
# HH $\rightarrow$ bbyy



	bb	WW	$\tau\tau$	ZZ	$\gamma\gamma$
bb	33%				
WW	25%	4.6%			
$\tau\tau$	7.4%	2.5%	0.39%		
ZZ	3.1%	1.2%	0.34%	0.076%	
$\gamma\gamma$	0.26%	0.10%	0.029%	0.013%	0.0005%

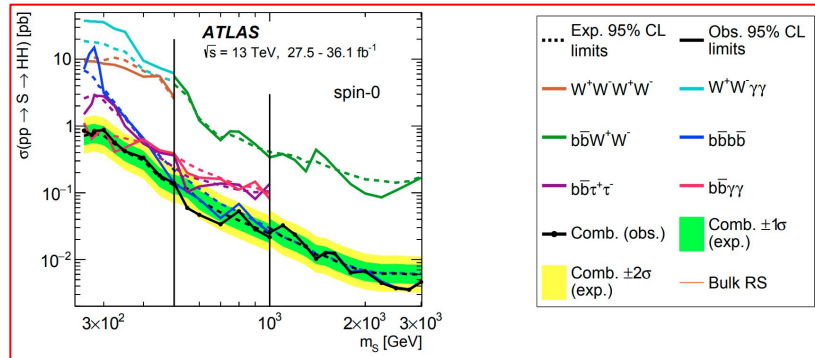
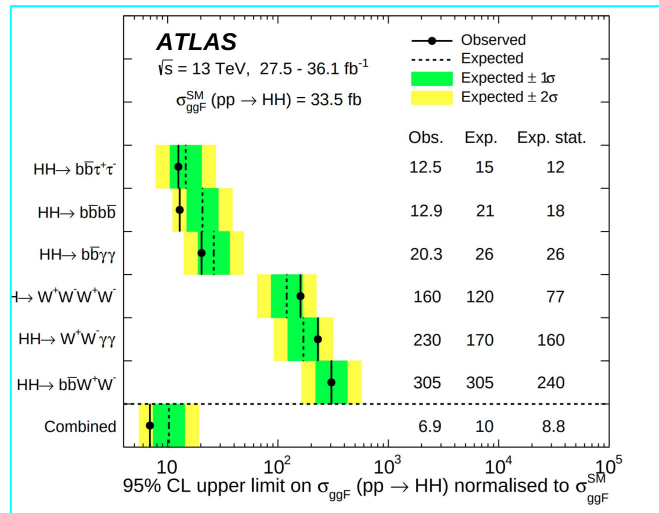


Clean and easy to trigger for low  $m_{HH}$



High signal rate

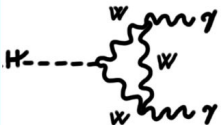
Previous: [HH combination 36.1 fb<sup>-1</sup>](#)



Current analysis: 139 fb<sup>-1</sup>  
 expect better sensitivities

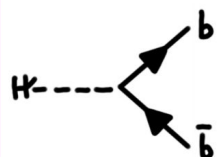
# Common preselection

- **Di-photons trigger:** efficiency: **82.9%** for SMHH; **69.5%** for  $m_X=300$  GeV
  - HLT\_g35\_loose\_g25\_loose (2015-2016)
  - HLT\_g35\_medium\_g25\_medium\_L12EM20VH (2017-2018)



At least **2 photons**:

- Identified (Tight WP)
- Calo- and Track-isolated within a cone of  $\Delta R = 0.2$ 
  - $E_T^{iso} < 0.065 \cdot E_T$  and  $p_T^{iso} < 0.05 \cdot E_T$
- $105 \text{ GeV} < m_{\gamma\gamma} < 160 \text{ GeV}$
- $E_T/m_{\gamma\gamma} > 0.35$  and  $0.25$
- $\gamma\gamma$  vertex

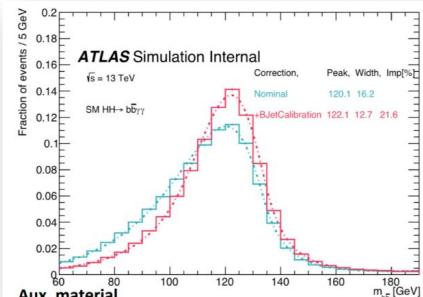


Less than 6 central jets (reduce ttH)

- PFlow jets, anti-kt R=0.4, tight JVT applied

Exactly **2 b-jets**

- DL1r 77% WP
- B-jet energy corrections applied →
  - Muon-in-jet
  - pT-reco

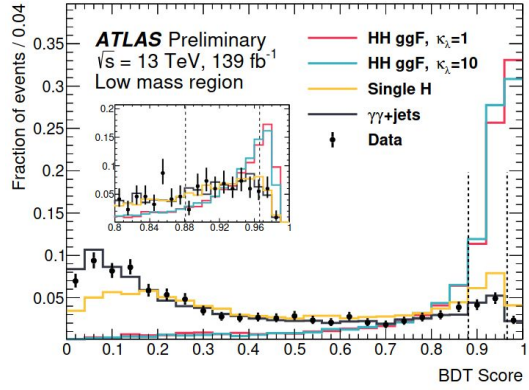
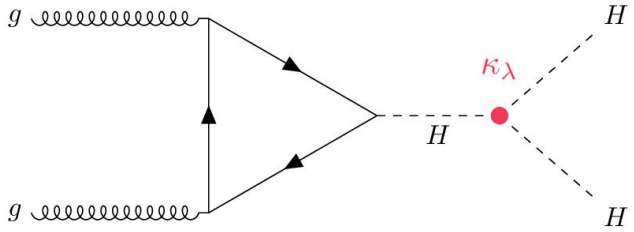


**Aux. material**

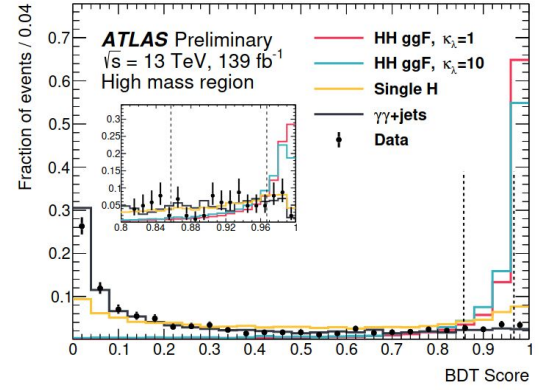
- **Lepton veto**

# Further selection with boosted decision tree (BDT)

Non-resonant analysis BDT:

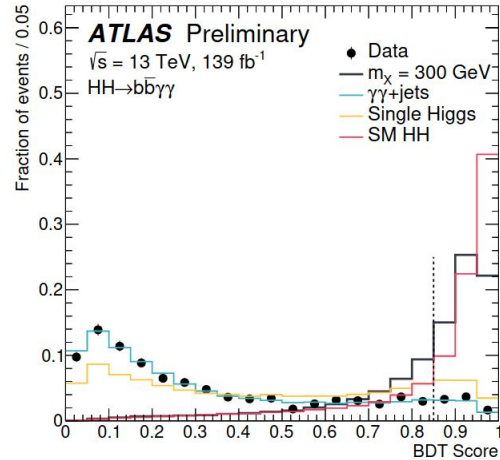
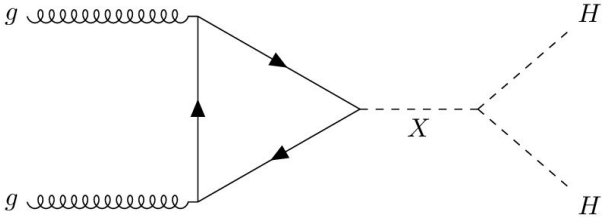


(a) Low mass region



(b) High mass region

Resonant analysis BDT:



BDTs trained with plenty of kinematics variables

# Statistical model (focus of my work)

Maximum likelihood fit performed on  $m_{\gamma\gamma} \in [105, 160]$  GeV, simultaneously with all the categories  
(Non-resonant: 4 cats; Resonant: 1 cat for each  $m_{\chi}$ )

## Likelihood

$$\mathcal{L} = \prod_c \left( \text{Pois}(n_c | N_c(\boldsymbol{\theta})) \cdot \prod_{i=1}^{n_c} f_c(m_{\gamma\gamma}^i, \boldsymbol{\theta}) \cdot G(\boldsymbol{\theta}) \right)$$

## Event parametrization

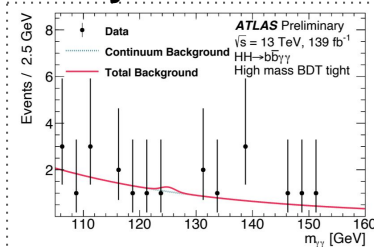
$$N_c(\boldsymbol{\theta}) = \mu \cdot N_{HH,c}(\boldsymbol{\theta}_{HH}^{\text{yield}}) + N_{\text{bkg},c}^{\text{res}}(\boldsymbol{\theta}_{\text{res}}^{\text{yield}}) + N_{SS,c} \cdot \boldsymbol{\theta}^{\text{SS},c} + N_{\text{bkg},c}^{\text{non-res}}$$

## Full model pdf

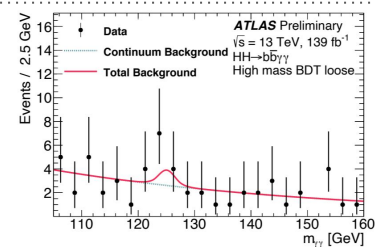
$$f_c(m_{\gamma\gamma}, \boldsymbol{\theta}) = [\mu \cdot N_{HH,c}(\boldsymbol{\theta}_{HH}^{\text{yield}}) \cdot f_{HH,c}(m_{\gamma\gamma}, \boldsymbol{\theta}_{HH}^{\text{shape}}) + N_{\text{bkg},c}^{\text{res}}(\boldsymbol{\theta}_{\text{res}}^{\text{yield}}) \cdot f_{\text{bkg},c}^{\text{res}}(m_{\gamma\gamma}, \boldsymbol{\theta}_{\text{res}}^{\text{shape}}) + N_{SS,c} \cdot \boldsymbol{\theta}_{HH}^{\text{SS},c} \cdot f_{HH,c}(m_{\gamma\gamma}, \boldsymbol{\theta}_{HH}^{\text{shape}}) + N_{\text{bkg},c}^{\text{non-res}} \cdot f_{\text{bkg},c}^{\text{non-res}}(m_{\gamma\gamma}, \boldsymbol{\theta}_{\text{non-res}}^{\text{shape}})] / N_c(\boldsymbol{\theta}_{\text{non-res}}^{\text{yield}})$$

## B-only fit

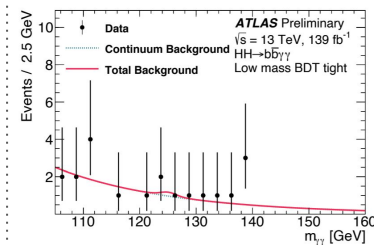
## Non-resonant



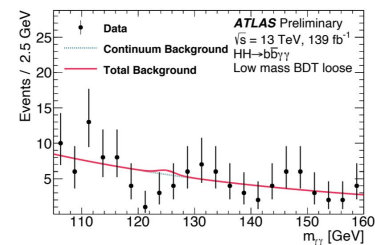
(a) High mass BDT tight



(b) High mass BDT loose

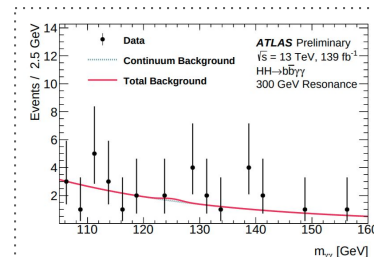


(c) Low mass BDT tight

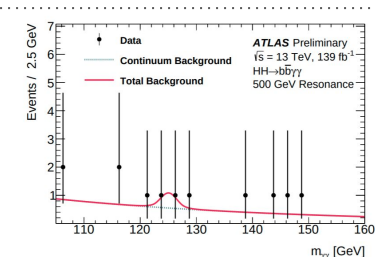


(d) Low mass BDT loose

## Resonant



(a)



(b)

# Non resonant results (focus of my work)

No signal observed, asymptotic limits with CLs have been derived for  $\mu_{\text{HH}, \kappa_\lambda=1}$  and  $\kappa_\lambda$

**95% CL limit on  $\mu_{\text{HH}}$  assuming  $\kappa_\lambda=1$ :**

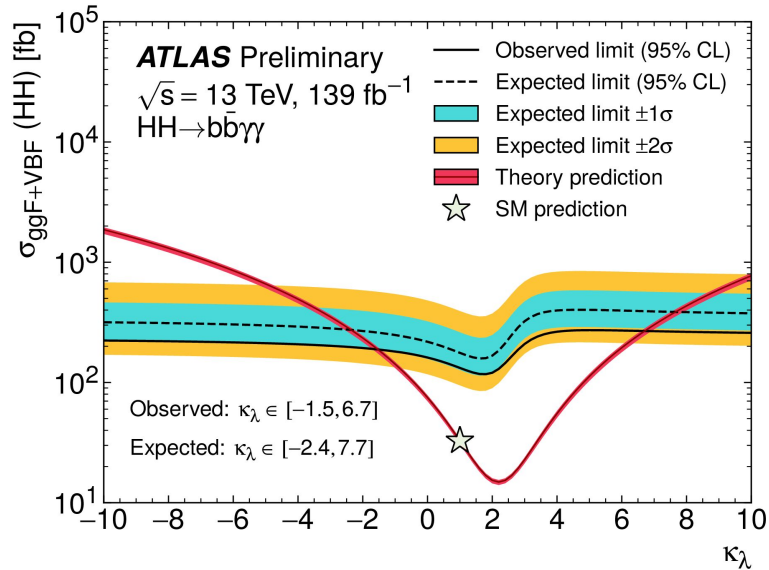
**obs: 4.1xSM** (22xSM with 36.1 fb<sup>-1</sup>)

**exp: 5.5xSM** (26xSM with 36.1 fb<sup>-1</sup>)

O(3%) systematic effect

A factor ~ 5 improvement:

- ~ 2 from increase of lumi
- ~ 2.5 from analysis



**95% CL limit on  $\kappa_\lambda$ :**

**obs: [-1.5, 6.7]** ([-8.2, 13.2] with 36.1 fb<sup>-1</sup>)

**exp: [-2.4, 7.7]** ([-8.3, 13.2] with 36.1 fb<sup>-1</sup>)

VBF HH contributes to an improvement of 5%

Full Run 2 CMS results:

**Limit of  $\mu_{\text{HH}}$ :**

**obs: 7.7xSM**

**exp: 5.2xSM**

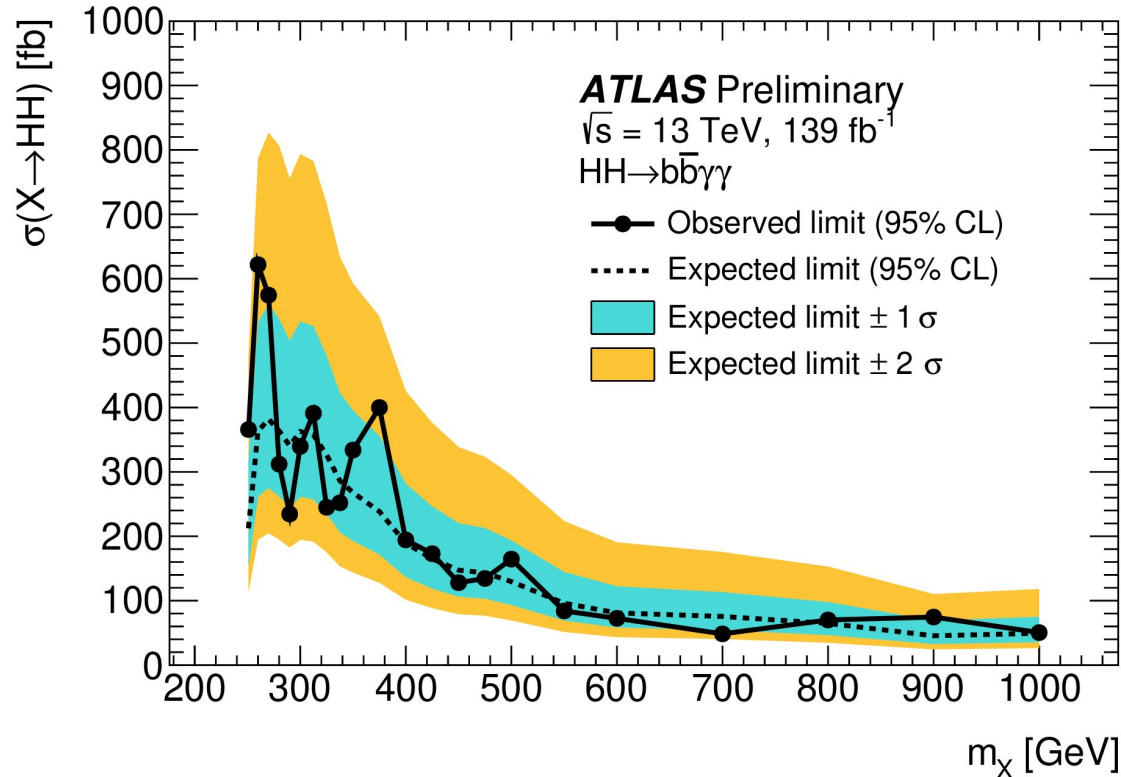
**Limit of  $\kappa_\lambda$ :**

**obs: [-3.3, 8.5]**

**exp: [-2.5, 8.2]**

# Resonant results

No signal observed, asymptotic limits with CLs on **cross section of each  $m_X$** :



factor  $\sim 2$  improvement w.r.t  $36.1 \text{ fb}^{-1}$   
factor  $\sim 1.2$  improvement from analysis



# Summary

## Calibration:

- In-situ calibration of ECAL with Zee events.
- Non-linearity energy response of ECAL

## HH→bbyy ATLAS Run2:

### Non-resonant:

- Improvement w.r.t. 36.1 fb<sup>-1</sup>
- Similar results with CMS

95% CL limit on  $\mu_{\text{HH},\kappa\lambda=1}$ :

obs: 4.1xSM

exp: 5.5xSM

95% CL limit on  $\kappa_\lambda$ :

obs: [-1.5, 6.7]

exp: [-2.4, 7.7]

### Resonant:

- Improvement w.r.t. 36.1 fb<sup>-1</sup>

95% CL limit on  $\sigma(\text{gg}\rightarrow\text{X}\rightarrow\text{HH})$ :

obs: 610–47 fb

exp: 360–43 fb

for  $251 \text{ GeV} \leq m_{\text{X}} \leq 1000 \text{ GeV}$

backup

# Data and MC

- Full Run 2 data (139 fb<sup>-1</sup>): [previous study with 36.1 fb<sup>-1</sup>](#)
- ggF HH signal ( $\kappa_\lambda = 1,10$ ) at NLO with Powheg-Box v2 + Pythia 8 +  $\kappa_\lambda$  reweighting technique
- VBF HH signal ( $\kappa_\lambda = 0,1,2,10$ ) at LO MadGraph5\_aMC@NLO v2.6.0 NNPDF3.0nlo + Pythia 8
  - Herwig 7 used for parton shower uncertainty
- Spin 0 resonance (251-1000 GeV) at LO with MadGraph5\_aMC@NLO v2.6.1 + Herwig v7.1.3
- Single Higgs and  $\gamma\gamma$ -continuum background :

Single Higgs and continuum bkg MC

Process	Generator	PDF set	Showering	Tune
ggF	NNLOPS [65–67] [68, 69]	PDFLHC [42]	PYTHIA 8.2 [70]	AZNLO [71]
VBF	POWHEG BOX v2 [39, 66, 72–78]	PDFLHC	PYTHIA 8.2	AZNLO
$WH$	POWHEG BOX v2	PDFLHC	PYTHIA 8.2	AZNLO
$qq \rightarrow ZH$	POWHEG BOX v2	PDFLHC	PYTHIA 8.2	AZNLO
$gg \rightarrow ZH$	POWHEG BOX v2	PDFLHC	PYTHIA 8.2	AZNLO
$t\bar{t}H$	POWHEG BOX v2 [73–75, 78, 79]	NNPDF3.0nlo [80]	PYTHIA 8.2	A14 [81]
$bbH$	POWHEG BOX v2	NNPDF3.0nlo	PYTHIA 8.2	A14
$tHqj$	MADGRAPH5_aMC@NLO	NNPDF3.0nlo	PYTHIA 8.2	A14
$tHW$	MADGRAPH5_aMC@NLO	NNPDF3.0nlo	PYTHIA 8.2	A14
$\gamma\gamma$ +jets	SHERPA v2.2.4 [56]	NNPDF3.0nlo	SHERPA v2.2.4	–
$t\bar{t}\gamma\gamma$	MADGRAPH5_aMC@NLO	NNPDF2.3lo	PYTHIA 8.2	–

# Prediction of different $\kappa_\lambda$ with reweighting technique

$$A(k_t, k_\lambda) = k_t^2 B + k_t k_\lambda T. \quad (1)$$

319 The amplitude square is written as:

$$|A(k_t, k_\lambda)|^2 = k_t^4 |B|^2 + k_t^2 k_\lambda^2 |T|^2 + k_t^3 k_\lambda (B^* T + B T^*). \quad (2)$$

320 The amplitude square can be further expressed in terms of the amplitude squares of three reference samples  
 321 chosen. In this analysis, the reference samples are chosen to be  $k_\lambda = 0, 1, 10$  samples. Since we are only  
 322 interested in  $k_\lambda$ ,  $k_t$  is taken as 1.

$$|A(1, 0)|^2 = |B|^2, \quad (3)$$

$$|A(1, 1)|^2 = |B|^2 + |T|^2 + (B^* T + B T^*) \quad (4)$$

$$|A(1, 10)|^2 = |B|^2 + 100|T|^2 + 10(B^* T + B T^*) \quad (5)$$

323 Using these equations,  $|A(k_t, k_\lambda)|^2$  can be expressed in terms of amplitude squares of the three reference  
 324 samples.

$$|A(k_t, k_\lambda)|^2 = k_t^2 \left[ \frac{90k_t^2 + 9k_\lambda^2 - 99k_t k_\lambda}{90} |A(1, 0)|^2 + \frac{100k_t k_\lambda - 10k_\lambda^2}{90} |A(1, 1)|^2 + \frac{k_\lambda^2 - k_t k_\lambda}{90} |A(1, 10)|^2 \right] \quad (6)$$

Description from previous [36.1 fb<sup>-1</sup> note](#).

Linear combination of 3  $\kappa_\lambda$  samples for generation of other values of  $\kappa_\lambda$

Event-level weight applied on  $m_{\text{HH}}$  kinematics

For current Run 2 analysis,  $\kappa_\lambda = 0, 1, 20$  are used.

Systematic uncertainty estimated with differences between generated and reweighted samples at  $\kappa_\lambda = 10$ .

# Non resonant BDT input variables

Table 2: Variables used in the BDT for the non-resonant analysis. The  $b$ -tag status identifies the highest fixed  $b$ -tag working point (60%, 70%, 77%) that the jet passes. All vectors in the event are rotated so that the leading photon  $\phi$  is equal to zero.

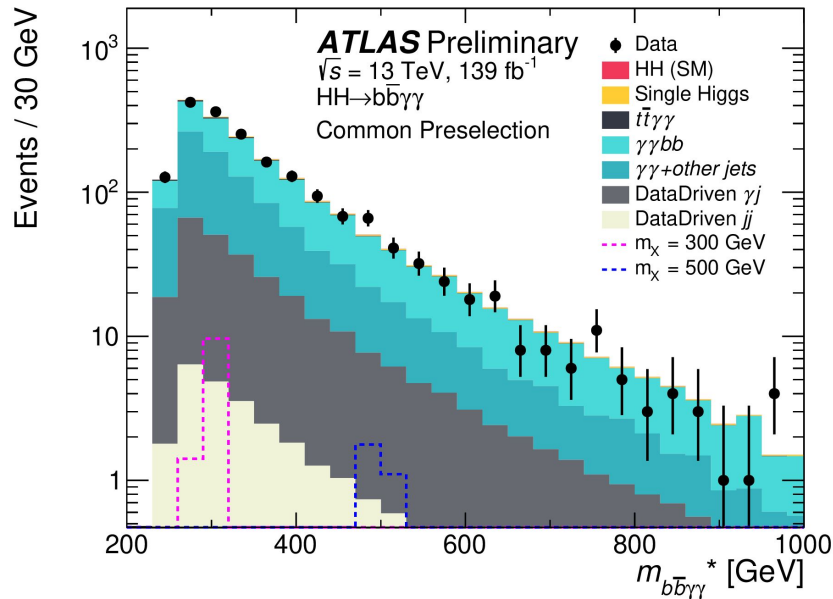
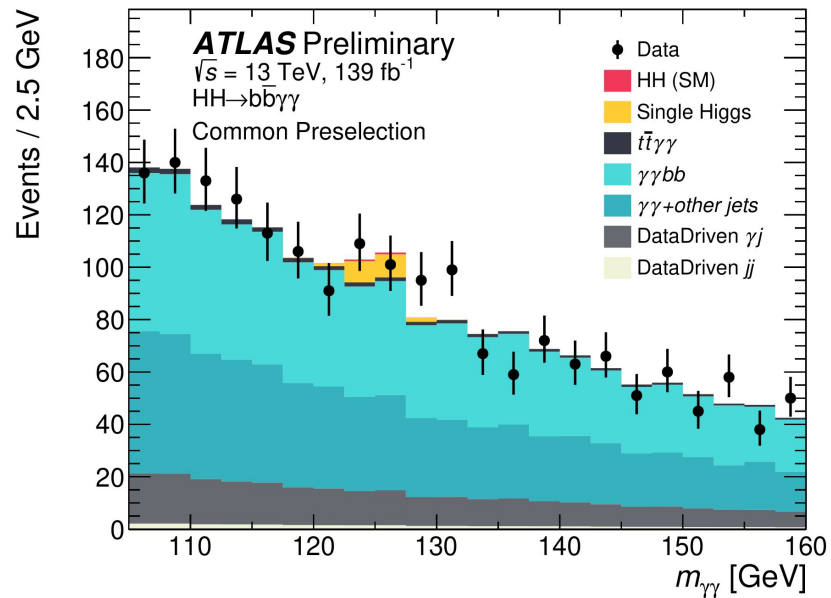
Variable	Definition
Photon-related kinematic variables	
$p_T/m_{\gamma\gamma}$	Transverse momentum of the two photons scaled by their invariant mass $m_{\gamma\gamma}$
$\eta$ and $\phi$	Pseudo-rapidity and azimuthal angle of the leading and sub-leading photon
Jet-related kinematic variables	
$b$ -tag status	Highest fixed $b$ -tag working point that the jet passes
$p_T, \eta$ and $\phi$	Transverse momentum, pseudo-rapidity and azimuthal angle of the two jets with the highest $b$ -tagging score
$p_T^{b\bar{b}}, \eta_{b\bar{b}}$ and $\phi_{b\bar{b}}$	Transverse momentum, pseudo-rapidity and azimuthal angle of $b$ -tagged jets system
$m_{b\bar{b}}$	Invariant mass built with the two jets with the highest $b$ -tagging score
$H_T$	Scalar sum of the $p_T$ of the jets in the event
Single topness	For the definition, see Eq. (1)
Missing transverse momentum-related variables	
$E_T^{\text{miss}}$ and $\phi^{\text{miss}}$	Missing transverse momentum and its azimuthal angle

# Resonant BDT input variables

Table 4: Variables used in the BDT for the resonant analysis. For variables depending on  $b$ -tagged jets, only jets  $b$ -tagged using the 77% working point are considered as described in Section 4.1.

Variable	Definition
Photon-related kinematic variables	
$p_{\text{T}}^{\gamma\gamma}, y^{\gamma\gamma}$	Transverse momentum and rapidity of the di-photon system
$\Delta\phi_{\gamma\gamma}$ and $\Delta R_{\gamma\gamma}$	Azimuthal angular distance and $\Delta R$ between the two photons
Jet-related kinematic variables	
$m_{b\bar{b}}, p_{\text{T}}^{b\bar{b}}$ and $y_{b\bar{b}}$	Invariant mass, transverse momentum and rapidity of the $b$ -tagged jets system
$\Delta\phi_{b\bar{b}}$ and $\Delta R_{b\bar{b}}$	Azimuthal angular distance and $\Delta R$ between the two $b$ -tagged jets
$N_{\text{jets}}$ and $N_{b\text{-jets}}$	Number of jets and number of $b$ -tagged jets
$H_{\text{T}}$	Scalar sum of the $p_{\text{T}}$ of the jets in the event
Photons and jets-related kinematic variables	
$m_{b\bar{b}\gamma\gamma}$	Invariant mass built with the di-photon and $b$ -tagged jets system
$\Delta y_{\gamma\gamma, b\bar{b}}, \Delta\phi_{\gamma\gamma, b\bar{b}}$ and $\Delta R_{\gamma\gamma, b\bar{b}}$	Distance in rapidity, azimuthal angle and $\Delta R$ between the di-photon and the $b$ -tagged jets system

# Data vs MC: preselection

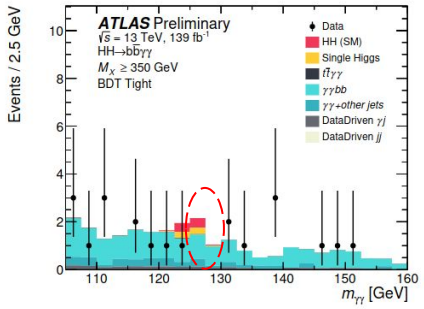


$$m_{b\bar{b}\gamma\gamma}^* = m_{bb\gamma\gamma} - m_{bb} - m_{\gamma\gamma} + 250 \text{ GeV}$$

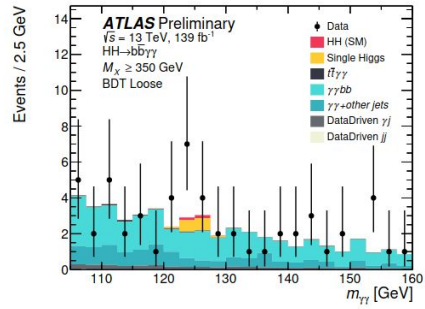
improve resolution with correlations

# Data vs MC: diphoton mass spectrum

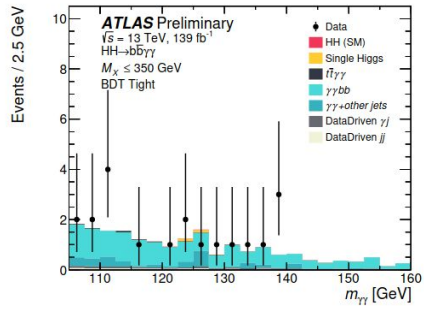
## Non-resonant



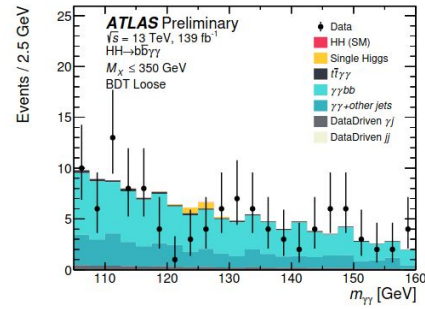
(a) High mass BDT tight selection



(b) High mass BDT loose selection

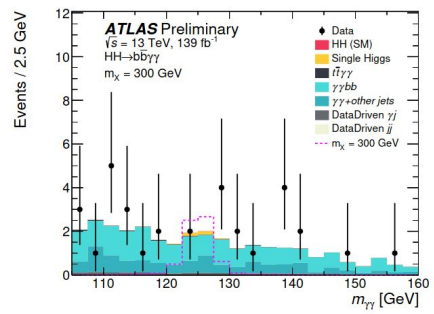


(c) Low mass BDT tight selection

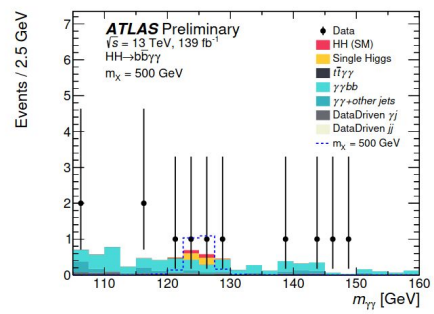


(d) Low mass BDT loose selection

## Resonant



(a)



(b)

yybb: dominant background  
 Data-driven yj, jj via 2x2D (y: isolation and ID)  
 Single Higgs: ttH, ZH, ggH dominant  
 (all single Higgs modes involved)



# Cut flow HH

## Non-resonant

Cuts	raw number of events	Yield	Efficiency
$N_{xAOD}$	1.56e+06	11.3696	100
$N_{DxAOD}$	1.56e+06	11.3696	100
All events	1.56e+06	11.3685	99.9903
No duplicates	1.56e+06	11.3685	99.9903
GRL	1.56e+06	11.3685	99.9903
Pass trigger	1.30292e+06	9.43463	82.9808
Detector DQ	1.30292e+06	9.43463	82.9808
Has PV	1.30292e+06	9.43463	82.9808
2 loose photons	962029	7.00497	61.6112
$e - \gamma$ ambiguity	961632	7.00186	61.5838
Trigger match	913938	6.65969	58.5743
tight ID	799960	5.85507	51.4974
isolation	709300	5.16719	45.4472
$rel.p_T cuts$	638923	4.64775	40.8786
$m_{\gamma\gamma} \in [105, 160]$	638541	4.64498	40.8542
$N_{lep} = 0$	638371	4.71206	41.4442
$N_j > 2$	635973	4.69411	41.2863
$N_j$ central <6	540328	3.94838	34.7274
leading jet 85% WP	521719	3.81785	33.5793
subleading jet 85% WP	269007	2.01101	17.6875
$N_{j btag} < 3$	263071	1.96522	17.2847
2 b-jet with 77% WP	210794	1.56478	13.7628
DiHiggs invariant mass <350	23434	0.187622	1.6502
DiHiggs invariant mass >350	187360	1.37716	12.1126

Table 152: Cutflow for Non resonant  $x \rightarrow hh \rightarrow \nu y b b$

## Resonant

Cuts	raw number of events	Yield	Efficiency
$N_{xAOD}$	820000	133.994	100
$N_{DxAOD}$	820000	133.994	100
All events	820000	133.985	99.9927
No duplicates	820000	133.985	99.9927
GRL	820000	133.985	99.9927
Pass trigger	561153	91.8438	68.543
Detector DQ	561153	91.8438	68.543
Has PV	561153	91.8438	68.543
2 loose photons	461295	75.6471	56.4554
$e - \gamma$ ambiguity	461105	75.6125	56.4296
Trigger match	415412	68.3971	51.0447
tight ID	354968	58.6712	43.7863
isolation	299286	49.2099	36.7254
$rel.p_T cuts$	270121	44.4441	33.1686
$m_{\gamma\gamma} \in [105, 160]$	269966	44.419	33.1499
$N_{lep} = 0$	269872	45.2723	33.7867
$N_j > 2$	268619	45.0653	33.6322
$N_j$ central <6	201307	33.2857	24.8411
leading jet 85% WP	199795	33.0534	24.6677
subleading jet 85% WP	90129	14.7167	10.9831
$N_{j btag} < 3$	88730	14.4868	10.8115
2 b-jet with 77% WP	70698	11.289	8.42498
DiHiggs invariant mass selection	70698	11.289	8.42498
BDT selection	40764	6.52261	4.86782
$m_{\gamma\gamma} \in [120, 130]$	38981	6.24486	4.66053

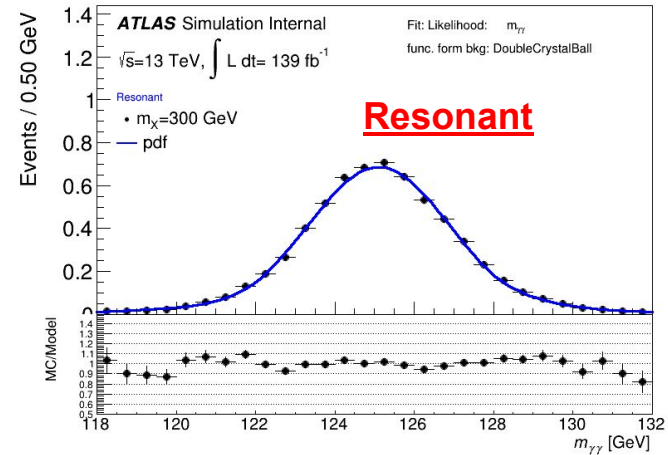
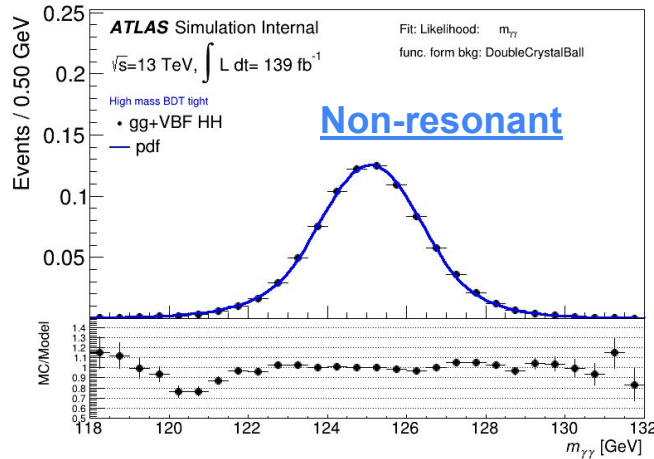
Table 158: Cutflow for resonant  $x_{300} \rightarrow hh \rightarrow \nu y b b$

# Signal and background modeling

$m_{\gamma\gamma}$  used as final discriminant variable for both non-resonant and resonant analysis

**HH signal** and **single Higgs background** modeled with the same **DSCB** function

HH yields  $f(\kappa_\lambda)$  parametrized with **2nd order polynomial**, single Higgs yields fixed to **SM prediction**



**Continuum background** modelled with **exponential** function:

Low  $\gamma\gamma$ -continuum MC statistic

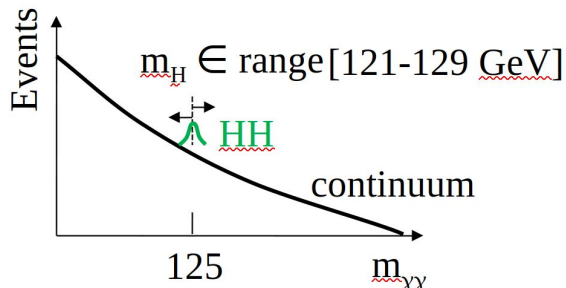
- Exponential checked by Wald test on data: no preference of higher degree function
- S+B fit on b-only template to compute uncertainty of **spurious signal**

**Injection test:** bias up to 10% (5%) for non-resonant (resonant) analysis

# Background modeling and spurious signal

## S+B fit on b-only MC templates:

-Spurious signal:  $N_{sp} = \max |n_{sig}(m_H)|$



Non-resonant

Category	$n_{sp}$	$Z_{spur}$	$p(\chi^2)[\%]$
High mass BDT tight	0.688	0.394	68.8
High mass BDT loose	0.990	0.384	30.5
Low mass BDT tight	0.594	0.378	29.8
Low mass BDT loose	1.088	0.272	26.9

Signal mass [GeV]	$n_{sp}$	$Z_{spur}$	$p(\chi^2)[\%]$
251	0.269	0.179	97
260	0.787	0.277	1
270	1.057	0.431	-
280	0.561	0.245	0
290	0.620	0.272	-
300	0.938	0.421	0
312.5	0.538	0.223	-
325	1.075	0.470	0
337.5	0.819	0.399	-
350	0.832	0.457	7
375	0.382	0.303	-
400	0.295	0.182	0
425	0.378	0.310	-
450	0.451	0.421	1
475	0.758	0.594	-
500	0.218	0.178	0
550	0.140	0.155	31
600	0.095	0.115	19
700	0.532	0.397	0
800	0.150	0.152	0
900	0.213	0.286	97
1000	0.269	0.304	71

Resonant

- **Relaxed Criteria:** lack bkg MC statistics  
if  $N_{sp} > 2\Delta n_{sig}^{MC stat}$  then  $\zeta_{sp} = N_{sp} - 2\Delta n_{sig}^{stat MC}$   
else  $\zeta_{sp} = 0$

Pass OR of:  $-\zeta_{sp} < 10\% N_{signal}$  expected

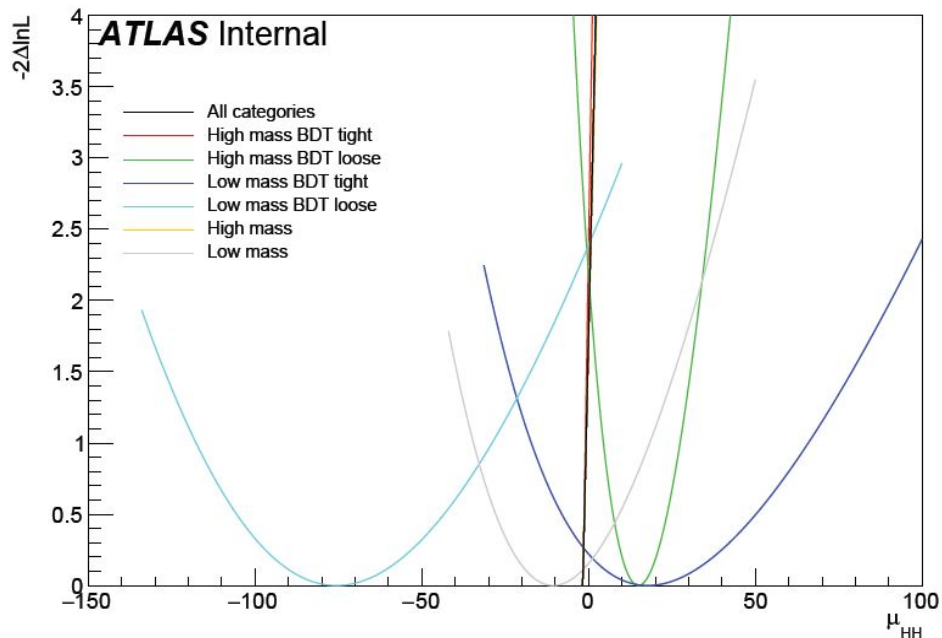
$-\zeta_{sp} < 20\% \sigma_{bkg}$ , ( $Z_{sp} < 20\%$ )

- **Wald test** on real blinded data

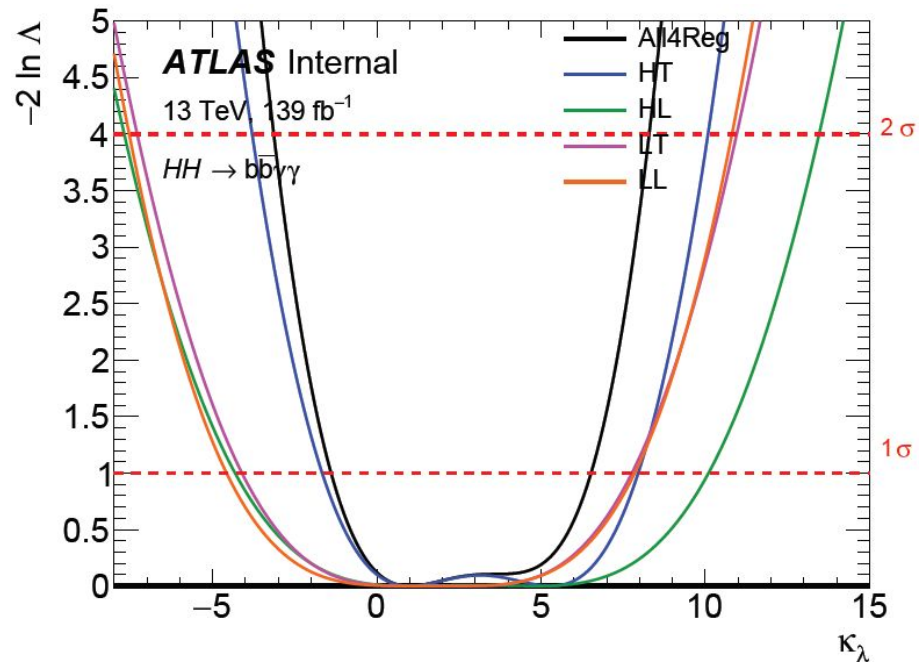
**Stick to natural form : exp**

# Non-resonant likelihood scan

Likelihood scan on  $\mu$ , with  $\kappa_\lambda=1$

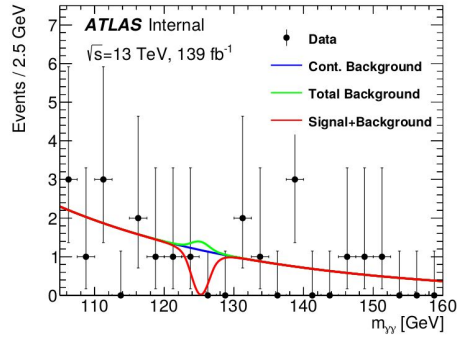


Likelihood scan on  $\kappa_\lambda$ , with  $\mu=1$

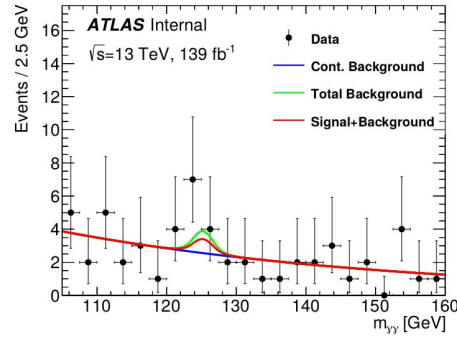


Likelihood performed simultaneously and individually with all the categories

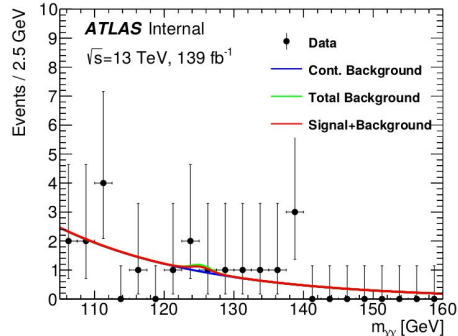
# Non-resonant S+B fit



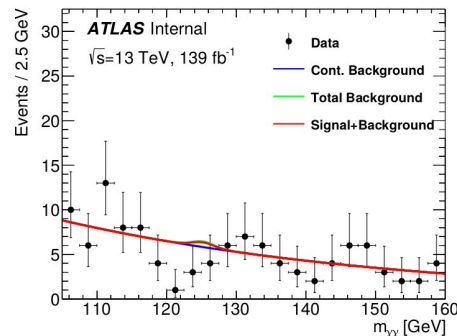
(a) High mass BDT tight



(b) High mass BDT loose



(c) Low mass BDT tight



(d) Low mass BDT loose

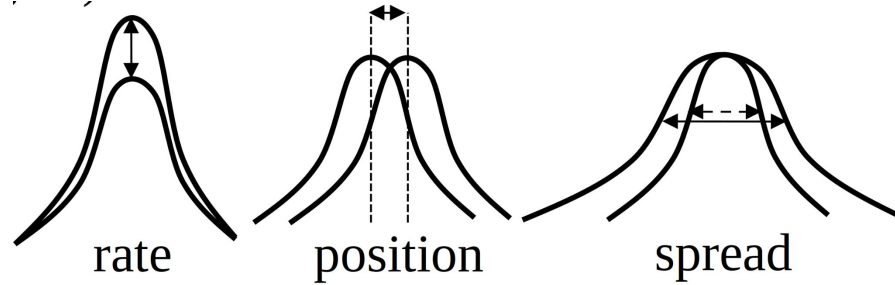
Due to the **large deficit** in the **High mass BDT tight category** (most sensitive), a negative signal strength ( $\mu \approx -2$ ) has been observed

Figure 45: The observed data fitted with the signal + background model, in the four non-resonant ggF categories.

# Systematic uncertainties

Systematic uncertainties:

- **Event rate**
- **Shape of  $m_{\gamma\gamma}$** 
  - signal pdf (DSCB)
  - spurious signal from bkg



		Relative impact of the systematic uncertainties in %	
Source	Type	Non-resonant analysis <i>HH</i>	Resonant analysis $m_X = 300$ GeV
Experimental			
Photon energy scale	Norm. + Shape	5.2	2.7
Photon energy resolution	Norm. + Shape	1.8	1.6
Flavor tagging	Normalization	0.5	< 0.5
Theoretical			
Heavy flavor content	Normalization	1.5	< 0.5
Higgs boson mass	Norm. + Shape	1.8	< 0.5
PDF+ $\alpha_s$	Normalization	0.7	< 0.5
Spurious signal	Normalization	5.5	5.4

## Experimental systematics

photon, jets, b-tagging ...

## Theoretical systematics

- QCD, pdf+ $\alpha_s$
- HF (100 %) [ggH, VBF, WH]
- BRs,  $m_{top}$
- Parton Showering (H7 vs Py8)
- $\kappa_\lambda$  reweighting syst (O(5 %))

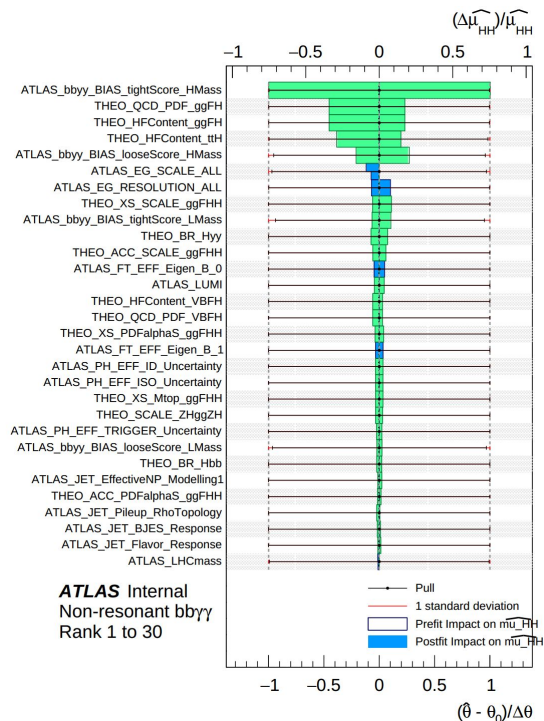


# Ranking of systematic: expected

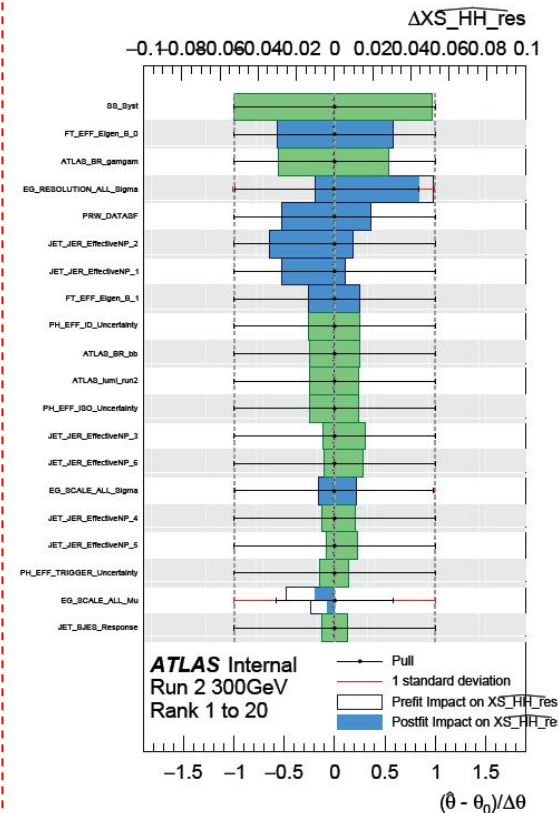
**Asimov dataset :**  
syst. profiled from bkg-only fit  
+ add  $\mu_{HH}=1$  (SM)

Dominant systematic :  
**-spurious signal**  
**-HF in ggH**

## Non-resonant



## Resonant



# Narrow width approximation: scalar

$$\frac{1}{(s - M^2)^2 + M^2\Gamma^2} \xrightarrow{\Gamma/M \rightarrow 0} \frac{\pi}{M\Gamma} \delta(s - M^2)$$

$$\lim_{\epsilon \rightarrow 0} \frac{\epsilon}{\epsilon^2 + x^2} = \pi\delta(x)$$

$$\frac{1}{\Gamma M^3} \frac{\Gamma/M}{(s/M^2 - 1)^2 + (\Gamma/M)^2} \rightarrow \frac{1}{\Gamma M^3} \pi\delta(s/M^2 - 1) = \frac{1}{\Gamma M} \pi\delta(s - M^2)$$

Narrow width approx. allows to write the propagator (w/ decay width) as dirac function and  $1/\text{decay\_width}$ .

Dirac function: on-shell particle  $\rightarrow$  off-shell dropped

$1/\text{decay\_width}$ : cross section = production cross section \* BR



# Non resonant results: toys vs asymptotic

For **SM HH signal strength  $\mu$** , toys have been studied for the validation of asymptotic formula, for both **stat-only** and **full model**

<b>stat-only</b>	<b>exp</b>	<b>obs</b>
<u>Asymptotic</u>	5.314	3.787
<u>Toys 100k</u>	5.342	3.952
<u>difference</u>	0.5%	4.4%

<b>full-model</b>	<b>exp</b>	<b>obs</b>
<u>Asymptotic</u>	5.465	4.089
<u>Toys 50k</u>	5.912	4.237
<u>difference</u>	8.2%	3.6%

\*stat-only limits derived by simply setting all NPs to 0 in the model

**stat-only:** bias up to 4%

**full model:** for expected, bias increased to 8%

<https://indico.cern.ch/event/1016128/contributions/4300571/>  
<https://indico.cern.ch/event/1028088/contributions/4320759/>